Nb_3Sn CAVITIES: MATERIAL CHARACTERIZATION AND COATING PROCESS OPTIMIZATION*

D.L. Hall, T. Gruber, J.J. Kaufman, M. Liepe, J.T. Maniscalco, S. Posen†, B. Yu
Cornell Laboratory for Accelerator-Based Sciences and Education (CLASSE),
Ithaca, NY 14853, USA
T. Proslier
Argonne National Laboratory, Argonne, Illinois 60439, USA

Abstract

Recent progress on vapour diffusion coated Nb_3Sn SRF cavities makes this material a very promising alternative for CW medium field SRF applications. In this paper we report on several systematic studies to determine the sources currently limiting the performance of Nb_3Sn cavities to determine improved coating parameters to overcome these limitations. These include a detailed study of the sensitivity of Nb_3Sn to trapped ambient magnetic flux, a first measurement of the field dependence of the energy gap in Nb_3Sn and detailed measurements of the stoichiometry of the obtained Nb_3Sn coatings with synchrotron x-ray diffraction and STEM. Initial results from a study on the impact of the coating process parameters on energy gap, Q-slope, and residual resistance, show clear dependencies, and thus directions for process optimization.

INTRODUCTION

Cornell's cutting-edge program on the development of Nb_3Sn-on-Nb cavities as an alternative to bulk niobium has produced cavities that do not suffer from the Q-slope endemic to previous attempts [1–3]. Recent work on improving the quality factor of these cavities, as well as their susceptibility to ambient magnetic flux has resulted in a $Q_0 \approx 2 \times 10^{10}$ at 16 MV/m at 4.2 K [4]. Contemporarily, recent material studies [5] of the Nb_3Sn produced by the vapour deposition method have shown that the current limitations are non-fundamental, and are instead related to the fabrication process of the thin-film layer. In this paper we present the initial results of a systematic study that will attempt to connect the parameters utilised in the fabrication process to material characteristics and RF performance, with the ultimate objective of creating a map between the two that can be used to tailor the fabrication process to achieve the desired RF performance.

THE COATING PROCESS

The Cornell Nb_3Sn Furnace

Although a more in-depth description of the coating furnace and associated process is given in Ref. [1], a short summary will be given here: The coating furnace consists of a niobium insert, into which the tin crucible, nucleation agent, and any items to be coated, are placed, as seen in Fig. 1. This insert is installed into a vertical UHV furnace chamber. Located at the base of the coating insert is a small cylinder, whose mouth is open to the interior of the insert, in which the tin crucible is placed. Mounted around this location is a second set of heating elements, which allow the temperature of the tin crucible – hereafter referred to as the *source* – to be maintained at an equal or higher temperature than that of the cavity or samples that are to be coated (whose location will hereafter be referred to as the *chamber*). This difference in temperature between the source and the chamber, ΔT, is a crucial element of the coating process.

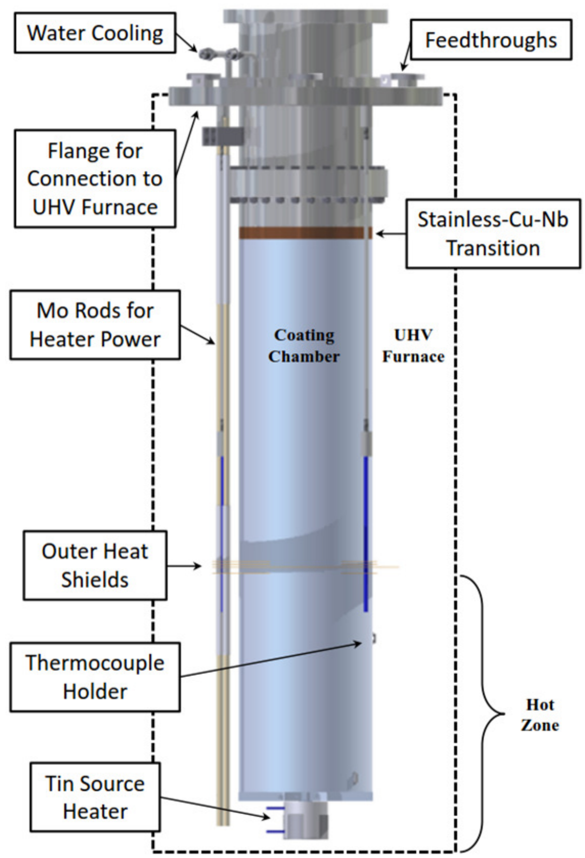

Figure 1: Diagram of the Cornell Nb_3Sn furnace coating insert from Ref. [1], highlighting the major elements.

* Work supported by DOE grant DE-SC0008431 and NSF grant PHY-141638. This work made use of the Cornell Center for Materials Research Shared Facilities which are supported through the NSF MRSEC program (DMR-1120296)

† Now at Fermi National Laboratory, Batavia, Illinois

ISBN 978-3-95450-178-6

The Coating Process

An example of the temperature profile for what is considered the standard coating recipe at Cornell is shown in Fig. 2. It should be noted that the temperatures seen in this profile are those of the thermocouples mounted inside the furnace, and that they do not equate to the temperature experience by source or chamber; a calibration curve is used to make that translation for the purposes of understanding what each of the two is subject to. Henceforth all temperatures cited here for the source and chamber are those that have been adjusted taking into account this calibration curve.

A standard coating consists of:

1. A degas stage lasting 24 hours,
2. **Nucleation** : both source and chamber held at 500°C for 5 hours,
3. **Ramp-up** : A ΔT of 100°C is created between source and chamber and the temperature is increased up to >1000°C for both, at an equal rate,
4. **Coating** : The chamber is held at 1100°C, and the source at 1200°C, for 3 hours,
5. **Annealing** : The source heater is turned off and the two temperatures are allowed to equilibrate; both the source and chamber are then kept at 1100°C for 6 hours before the furnace is turned off.

The furnace is then left to cool before the samples/cavity are removed.

VARIATIONS IN THE COATING PROCESS

Previously, very few variations in the time spent for each step have been attempted, and no variations in the temperatures had been performed at Cornell. For the purposes of this study, a single-cell 1.3 GHz fine-grain niobium cavity was coated four times, each time varying one parameter in the process:

- **Standard** : A standard coating as described in the previous section,
- **Extended coating** : The coating stage was extended to last 6 hours (c.f. 3),
- **Elevated coating** : The temperature of the source during the coating stage was elevated to 1230°C (c.f. 1200),
- **Elevated annealing** : The temperature of both the source and the chamber were elevated to 1200°C during the annealing stage (c.f. 1100°C).

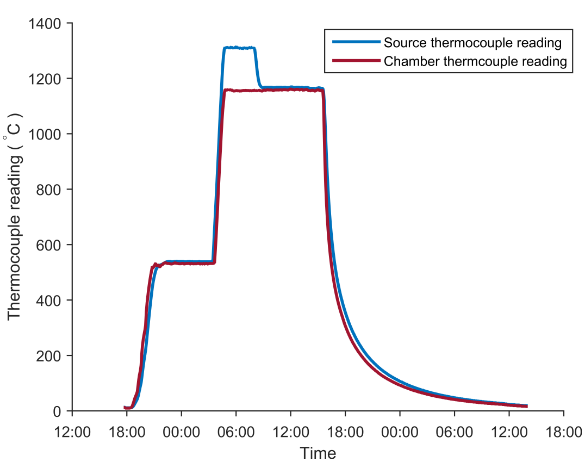

Figure 2: Temperature vs. time profile for a standard coating. The temperatures shown are for the thermocouples mounted inside the furnace and must be altered using a known calibration curve to obtain the temperatures of the tin crucible and cavity/samples to be coated.

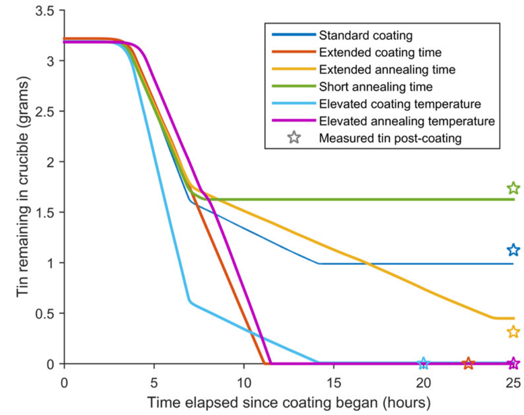

Figure 3: A simulation of the amount of tin remaining in the crucible as a function of time, taken from the end of the nucleation stage onwards, for different variations on the coating process. The simulation agrees well with the measured final tin amount, within 5% for all coatings.

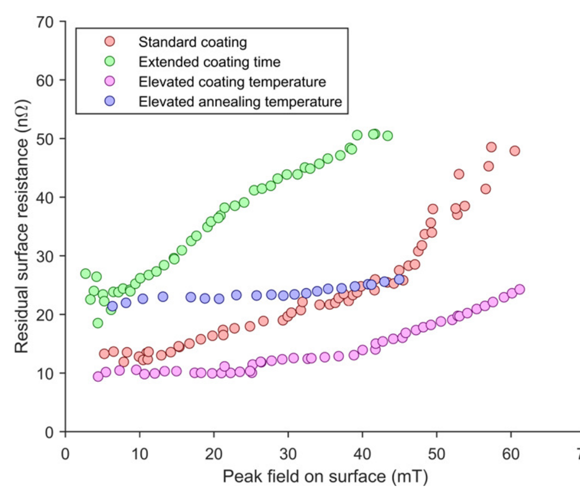

Figure 4: Residual resistance as a function of peak RF field on the surface of the cavity for different coating recipes performed on the same cavity. In each case, the maximum field achieved in the cavity was limited by a quench.

Between each coating, the cavity was tested and then the surface was reset, by doing a 10 minute inside-and-out cold BCP and a 20 minute inside-only cold BCP to remove the Nb_3Sn layer.

Recently, a simulation framework capable of calculating the evaporation rate of the tin in the crucible with temperature and time spent in the furnace has been completed. An example of the simulation for a number of different coating runs, including those described above, is shown in Fig. 3. As can be seen, during runs in which there is still tin remaining in the crucible post-coating, the simulation agrees with the final measured amount within 5% or better. This simulation will now be used to tailor the amount of tin for the desired length and temperature of the coating step; as can be seen, during a standard coating the remaining tin is still being transferred, albeit at a lower rate, during the annealing stage.

INITIAL RESULTS

A plot of the low-field BCS energy gap for the different coatings is shown in Fig. 5. Although more statistics are necessary, initial results show that the coating parameters do dictate the superconducting properties of the thin-film layer. The mechanism that gives rise to this change is the scope for further work.

A plot of the residual resistance with peak RF magnetic field on the surface for the different coatings is shown in Fig. 4. Contemporary studies have shown that the Q_0 and Q-slope in Nb_3Sn cavities up to medium fields of 15 MV/m are dominated by the residual resistance [4]. Initial results show that coating parameters do affect both the low-field Q_0, the Q-slope, and the quench field.

As seen in Fig. 6, the residual resistance at low fields is negatively impacted by a slower transfer rate of too much tin. Although in the standard coating the transfer rate is similar to that seen in the elevated annealing, the amount of tin transferred is approximately half of that transferred in both the extended coating and elevated annealing cases. In the case of the elevated coating, more tin was transferred, but the higher rate and shorter mean free path of the gaseous tin appear to have a positive impact in spite of more tin being transferred. It is also likely that the larger amount of tin transferred in this case was offset by the annealing step, during which the rate of tin arriving at the surface is more than halved.

A similar picture is seen with regards to the Q-slope for each coating, as seen in Fig. 7. In this case, the Q-slope is defined to be the linear change in surface resistance at 2 K (thus, in the scenario in which residual resistance dominates) over the low-to-medium-field region of 20-40 mT, corresponding to approx. 5-10 MV/m in an ILC cavity. In this case, we see that the elevated annealing actually demonstrates the smallest Q-slope, although the standard and elevated coatings are

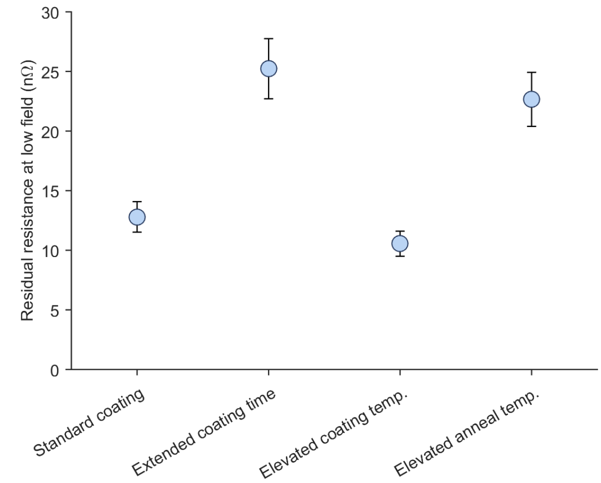

Figure 6: Residual resistance at low field for the four different coatings.

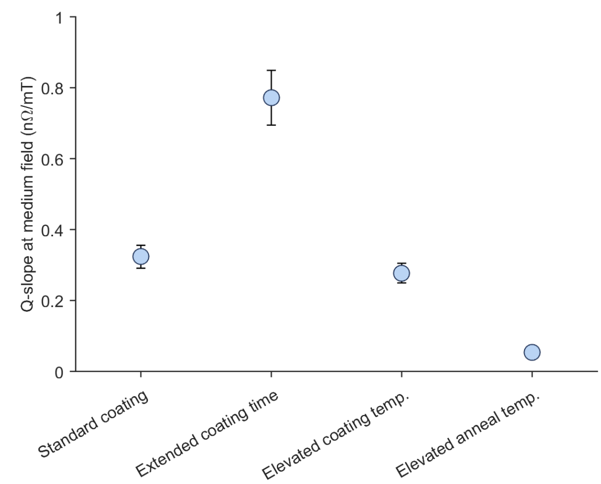

Figure 7: Q-slope – defined as change in surface resistance at 2 K per mT of applied RF magnetic field – for the four different coatings.

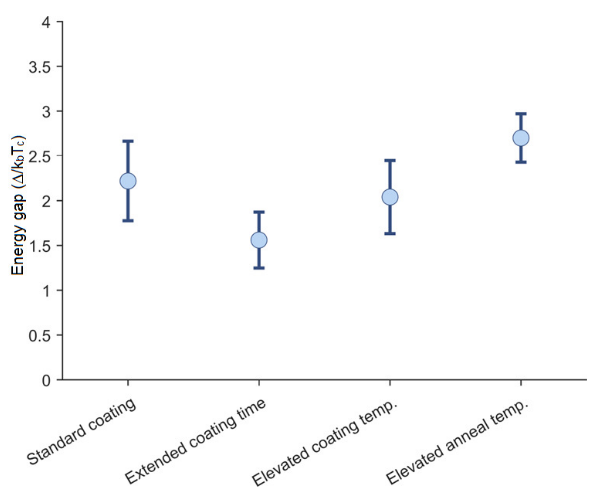

Figure 5: A plot of the energy gap at low field for the different coatings. At this stage the errors on the measurements are too large for decisive conclusions, but initial results do show that the coating parameters can affect the energy gap significantly.

ISBN 978-3-95450-178-6

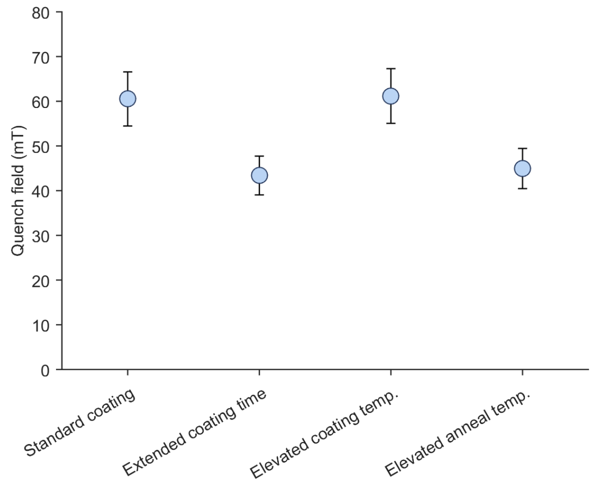

Figure 8: Measured Quench field at 2 K for the four different coatings.

also satisfactory. Once again, the transfer of more tin without any changes to the annealing stage or an increase in the rate of tin transfer, as was the case in the extended coating, is seen to have a negative impact on the cavity performance.

The final figure of merit is that of the quench field for each coating, see in Fig. 8. Here, we see two distinct cases: that of the extended coating and the elevated anneal, both of which quenched around 45 mT of peak RF magnetic field, and that of the standard and elevated coatings, both of which achieved 60 mT of peak RF field before quenching. This once again suggests that simply transferring more tin and/or over-annealing the cavity gives comparatively poor performance, and that a higher tin transfer rate and shorter tin mean free path, balanced against a correctly metered annealing stage, is key to good performance.

CONCLUSION

A systematic study of the effects of coating parameters on cavity performance has begun. This is being corroborated with material property studies carried out simultaneously [5]. Initial results suggest that the path to improved RF performance lies in a higher rate of transfer for the tin vapour, with a correspondingly lower mean free path, which likely results in a more even coating. Furthermore, it is evident that simply transferring more tin, and overdoing the annealing stage, are detrimental to the cavity's performance.

Further work will focus on changes in the amount of tin transferred during both the coating and annealing stages, utilising the simulation framework developed recently. Once complete, the resulting map of the parameter space will be utilised to develop a coating profile that maximises cavity efficiency and quench field.

REFERENCES

[1] Sam Posen. *Understanding and Overcoming Limitation Mechanisms in Nb_3Sn Supercomputing RF Cavities*. PhD thesis, Cornell University, 2014.

[2] Sam Posen and Matthias Liepe. Advances in development of Nb3Sn superconducting radio-frequency cavities. *Physical Review Special Topics - Accelerators and Beams*, 17(11):112001, November 2014.

[3] S. Posen, M. Liepe, and D. L. Hall. Proof-of-principle demonstration of Nb3Sn superconducting radiofrequency cavities for high Q0 applications. *Applied Physics Letters*, 106(8):082601, February 2015.

[4] Daniel Leslie Hall, Brian Clasby, Holly Conklin, Ralf Georg Eichhorn, Terri Gruber, Georg Hoffstaetter, John Julian Kaufman, and Matthias Liepe. High Quality Factor Studies in SRF Nb_3Sn Cavities. In *Proceedings of SRF 2015*, September 2015.

[5] Daniel Leslie Hall, Holly Conklin, Terri Gruber, John Julian Kaufman, James Maniscalco, Matthias Liepe, Byeonghee Yu, and Thomas Proslier. Surface Analysis and Material Property Studies of Nb_3Sn on Niobium for Use in SRF Cavities. In *Proceedings of SRF 2015*, September 2015.